

# Microstructure Evolution of Fine-Grained Cobalt T400 Tribaloy Processed by Spark Plasma Sintering or Hot Isostatic Pressing of Gas-Atomized Powders



X. BOULNAT, C. LAFONT, J.-B. COUDERT, and C. DAYOT

Tribaloys are Laves phases-hardened cobalt alloys usually produced by casting. In order to obtain a finer and more homogeneous microstructure, powder metallurgy was used by gas atomization of T400 Tribaloy powders followed by either spark plasma sintering (SPS) or hot isostatic pressing (HIP). Quantitative characterization of the microstructure was performed with X-ray diffraction, electron microscopy combined with energy-dispersive X-ray spectroscopy, at all stages of the processes. The gas atomized powder presents a fine composite microstructure composed of eutectic Laves phases and cobalt solid solution. The fraction of Laves phases increases upon consolidation time and temperature, with a composition tending to  $\text{Co}_3\text{Mo}_2(\text{Si} + \text{Cr})$ . This results in a hardness between 60 and 62 HRC for Spark Plasma Sintered and Hot Isostatic Pressed parts, depending on the consolidation parameters. The high solidification rates of atomization combined with powder consolidation lead to a fine-grained alloy, more homogeneous than cast alloys for the same grades.

<https://doi.org/10.1007/s11661-020-05962-3>

© The Minerals, Metals & Materials Society and ASM International 2020

## I. INTRODUCTION

IN order to increase the surface hardness of parts for wear applications, carburizing, nitriding or surface coating can be used.<sup>[1]</sup> Coating is applied by spraying high hardness alloy powders.<sup>[2–4]</sup> Cobalt base alloy powders of the Stellite or Tribaloy type are marketed for this type of application.<sup>[5,6]</sup> Instead, this project aims to develop a bulk material of this alloy by a powder metallurgy processing route. The alloy chosen is T400, from the Tribaloy family. These alloys exhibit very good wear resistance at high temperatures combined with good corrosion resistance.<sup>[1]</sup>

Tribaloys are cobalt alloys enriched in molybdenum and sometimes chromium, supplemented by a few percent Silicon (Table I). Their microstructure after casting consists of an intermetallic hard phase (Laves phase) dispersed in a softer matrix of eutectic solution (aggregate of a solid cobalt solution and Laves phases).<sup>[7]</sup> This principle of mechanical reinforcement by a hard phase in a ductile matrix is similar to Stellite alloys, which are reinforced by the presence of

chromium carbides ( $\text{M}_{23}\text{C}_6$ ,  $\text{M}_7\text{C}_3$ ).<sup>[8]</sup> These Stellites are therefore richer in chromium and carbon than Triballoys—for example Stellite 6 has 28 wt pct Cr and 1 pct wt carbon—and also exist in powder form and thus parts can be produced by HIP.<sup>[9,10]</sup>

The mechanical properties of Triballoys are highly dependent on the fraction of Laves phases.<sup>[11]</sup> The percentage of Laves phases, generally of composition  $\text{Co}_3\text{Mo}_2\text{Si}$  or  $\text{CoMoSi}$ , directly depends on the composition of the alloying elements Co, Mo, Si.<sup>[12,13]</sup> There are several types of Triballoys known as T100-T400-T800 whose fraction of Laves phases varies from 40 to 65 pct in volume. Chromium is placed in solid solution in the cobalt matrix but can sometimes substitute itself for silicon in the composition of the Laves phase.<sup>[12]</sup> Silicon plays a decisive role in the volume fraction of Laves phases.

T401 has less silicon but more chromium than T400, which reduces the fraction of Laves phases and thus increases the ductility of the material, but reduces hardness and wear resistance.<sup>[13]</sup>

This study focuses on the T400 alloy, whose microstructure and wear behavior are well documented for cast materials, making it possible to compare it with materials obtained by powder metallurgy. Powder metallurgy could be a way to avoid large heterogeneities found in cast alloys, such as segregation bands, and thus to improve bulk toughness when keeping a high level of hardness.

Two powder consolidation techniques will be used:

X. BOULNAT and C. LAFONT are with the Université de Lyon, INSA-Lyon, MATEIS UMR CNRS 5510, 69621 Villeurbanne, France. Contact e-mail: xavier.boulnat@insa-lyon.fr J.-B. COUDERT and C. DAYOT are with SKF Aerospace France, 22 Rue Brillat Savarin, 26300 Châteauneuf-sur-Isère, France.

Manuscript submitted November 26, 2019.

Article published online August 20, 2020

- (i) The flash sintering technique, or Spark Plasma Sintering (SPS), which makes it possible to obtain dense parts by unidirectional pressure and Joule heating of a powder contained in a graphite tool.
- (ii) Hot isostatic pressing (HIP), more commonly known in the industry, which consists of compacting under isostatic pressure (gas under pressure) a capsule in which the powder to be densified is contained.

The microstructures of these compacted billets and their resulting mechanical properties will be studied in order to compare them with the microstructural state and mechanical properties of Tribaloy alloys obtained by conventional casting.

## II. EXPERIMENTAL PROCEDURE

### A. Base Material: T400 Cobalt Alloy

The T400 powder was ordered from supplier Sandvik Osprey who could supply a batch of powders of a few kilograms. The atomization process was performed with nitrogen. The composition is given in Table II. It is to be noted:

- a high chromium content, which slightly exceeds the specifications with an upper limit set at 9.0 wt pct.
- a molybdenum content at 29.7 wt pct, very close to the upper limit of 30 wt pct.

These high contents will have an important role on the Laves phase fraction, as discussed later in the article.

### B. Processing Routes

The powder was then compacted in the SPS device HP D 25 of FCT Systeme Company. SPS compacts were cylindrical pellets of 20 mm diameter and 23 mm height

**Table I. Chemical Composition of Typical Triballoys**

Tribaloy	Co	Ni	Cr	Mo	Si	C
T100	bal.	< 1.5	—	35	10	< 0.08
T400	bal.	< 1.5	8.5	28.5	2.6	< 0.08
T800	bal.	< 1.5	17.5	28	3.4	< 0.08
T900	bal.	< 3.0	18	23	2.7	< 0.08
T401	bal.	—	17	22	1.2	< 0.08

**Table II. Chemical Analyses of T400 Performed by SANDVIK OSPREY LTD**

Composition (Wt Pct)	Co	Ni	Cr	Mo	Si	C	Mn	Fe
Min Spec.	bal.	0	7.0	27.0	2.0	0	0	0
T400-P	bal.	< 0.01	9.6	29.7	2.4	< 0.01	0.17	0.08
Max Spec	bal.	2.0	9.0	30.0	3.0	0.10	1.0	2.0

after compaction, which corresponds to a mass of 37 g of powders. An average sintering pressure of 76 MPa was applied. The latter was applied before heating at a rate of 100 K min<sup>-1</sup> up to the holding temperature (measured by pyrometry), which was chosen at 1323 K (1050 °C). The dwell time at maximum temperature was 10 minutes. Finally, cooling was induced by direct contact with water-cooled punches. Two compacts were made for each dwell temperature. The temperature given in this work was measured by a vertical pyrometer and tailored by an optimized PID controller.

HIPing cycles were performed at 1323 K (1050 °C) for 2 hours or at 1423 K (1150 °C) for 3 hours with a heating rate of 5 K min<sup>-1</sup> under an average pressure of 100 MPa. HIPed compacts were cylindrical parts of 60 mm diameter and 50 mm height.

### C. Characterization Methods

#### 1. Powder size distribution

A granulometric measurement of the powder was carried out at the MATEIS laboratory on the Malvern Mastersize 2000 device. The tests were carried out by dry method with a series of three measurements.

#### 2. Electron microscopy and energy-dispersive X-ray spectroscopy (EDX)

The powders and compacts were observed by field-emission scanning electron microscopy on a Zeiss Supra 55 VP SEM. The powders were deposited on a conductive carbon tape and observed in imaging under secondary electron mode (SE2 mode) at 10 kV or under backscattered electron mode (BSE), at 20 kV.

EDX mapping was performed under 20 or 25 kV on polished flat specimens.

#### 3. Quantification of phase fraction

In order to extract quantitative microstructural data, the fraction and size of each phase present in the powder was determined by SEM image analysis. The analysis procedure, performed with Fiji software, consisted in (i) optimizing the brightness/contrast (ii) thresholding the image to separate the two phases (iii) binarization (iv) quantitative fraction analysis using the « analyse particles » tool.

#### 4. X-ray diffraction

X-ray diffraction (XRD) patterns were recorded on atomized powders and bulk compacts with a Bruker D8 Advance X-ray Diffractometer, using the CuK ( $\lambda = 0.15418$  nm) radiation source. The  $2\theta$  range was from 35 to 55 deg and the scan rate was 0.3 deg min<sup>-1</sup>.

Vickers hardness testing was performed a load of 10 kgf on a Future Tech Vickers hardness tester. Rockwell C (HRC) measurements were performed using a load of 150 kgf on a WOLPERT machine. Both machines were verified in the corresponding loading range after NF EN ISO 6507-2 and NF EN ISO 6508-2, respectively.

Charpy impact tests were performed on a Tinius Olsen IT 503 device. The machine was not calibrated in the period of tests and the impact tests, performed at room temperature, were used for relative comparison between specimens only. No standard was applied.

### III. RESULTS AND DISCUSSION

#### A. Powder Characterization

The particle size distribution was measured by laser light diffraction. D10, D50 and D90 were found at 44, 72 and 119  $\mu\text{m}$ , respectively. The powders were observed by SEM (Figure 1).

A well spherical morphology of the powders is confirmed. However, there is very little presence of non-spherical powders: in sticks or in the form of several agglomerated powders during solidification at atomization. The microstructure of the powders is composed of (Figure 2):

- (i) Primary Laves phases (white contrast), of star or butterfly dendritic morphology, inherited from rapid solidification. These Laves phases are uniformly distributed in the powders, which indicates a good homogeneity of the powders.

- (ii) An eutectic aggregate of two phases: a solid solution phase of cobalt, in light gray, with which a finer Laves phase than the primary Laves phase is mixed.

A magnification  $\times 8000$  allows to visualize the details of the eutectic aggregate composed of the solid cobalt solution and the Laves (white) phase lamellae whose dimensions are less than one micron. This aggregate sometimes takes the form of a less distinct mixture of very fine Laves phases, in the order of 100 nm.

For comparison, the microstructure of a T400 raw casting alloy (as-cast) involved 33 to 42 pct vol of primary Laves phases surrounded by a eutectic aggregate composed of cobalt solid solution. The size of the Laves phases is smaller in the atomized powder than in the raw casting microstructure, whose size was found to be 6  $\mu\text{m}$  after arc melting + rapid cooling and 24 to 25  $\mu\text{m}$  after casting.<sup>[13,14]</sup>

Performed on 4 images from 4 different powder particles, the calculation of the percentage of Laves phase is  $51.3 \pm 2.9$  pct. This fraction includes the primary Laves phases and the Laves phases in the eutectic aggregate, of the same contrast. The fraction of Laves phases in T400 alloys is generally between 40 and 55 pct.<sup>[13]</sup> Being at the high end of the range is consistent with the chemical composition of the alloy, particularly the high molybdenum and silicon contents.

The chemical composition measurements were carried by EDX at the SEM:

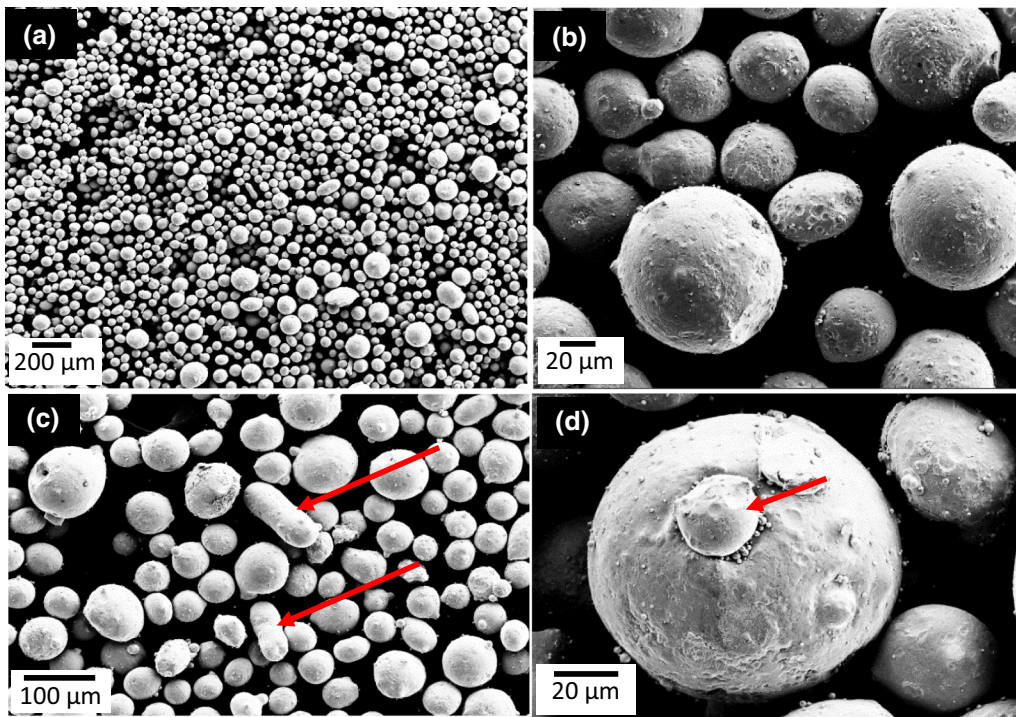


Fig. 1—SEM images (SE mode) at low (a) and high (b) magnification and with a focus on (c) elongated powders and (d) agglomerated satellites on a coarser powder.

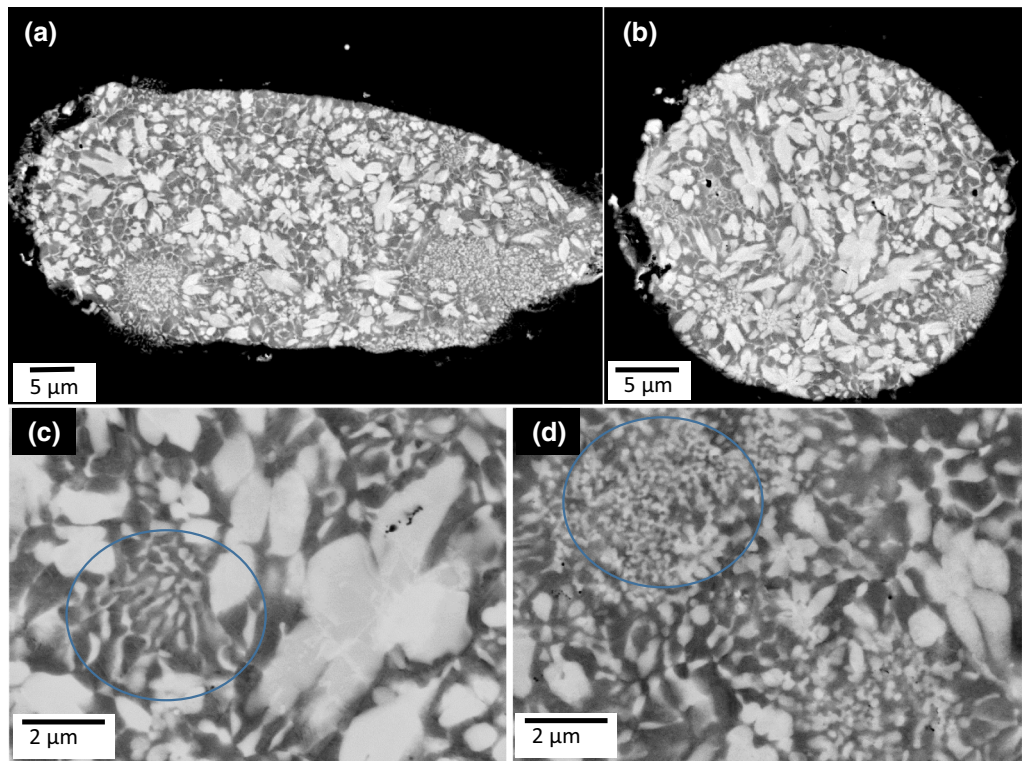


Fig. 2—SEM (AsB mode): microstructure of (a) an elongated powder, (b) a spherical powder, (c) focus on eutectic aggregate with lamellar Laves phases, (d) focus on eutectic aggregate with more isotropic Laves phases network.

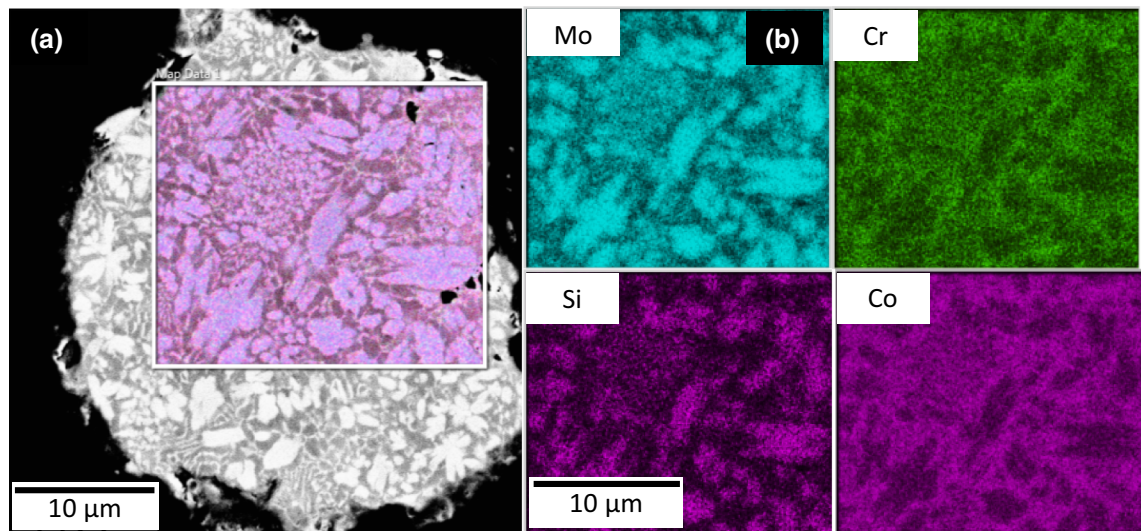


Fig. 3—(a) Area of powder particle analyzed by EDX. (b) Corresponding mapping of Mo, Cr, Si and Co contents (pixel intensity increases with content).

- a qualitative analysis to map differences in chemical composition in a given area. Figure 3 defines an area mapped by EDX overlaying the backscattered electron (AsB) contrast. The areas identified as Laves phases (white ASB contrast) are enriched with Mo and Si, two of the three elements composing the Laves phases (Figure 3). Conversely, Co and Cr elements are less present in the Laves phases than in the Cobalt solid solution.
- more quantitative analyses are carried out on an *ad hoc* basis by pointing to a particular element, for example, on each phase of the microstructure. For this type of analysis, 3 points are made on each phase type. These very local measurements (probe size of about  $1 \mu\text{m}^3$ ) allow the local composition of the two phases to be determined, as reported in Table III.

The Laves phases in the T400 have a composition ranging between CoMoSi and Co<sub>3</sub>Mo<sub>2</sub>Si.<sup>[14]</sup> Here, Cr is present not only in the cobalt solid solution at 12.2 wt pct, but also in the Laves phases at 7.5 wt pct. By summing the Cr and Si contents, stoichiometric proportions of the Laves phases are close to Co<sub>3</sub>Mo<sub>2</sub>(Si + Cr), which would correspond to 50 at. pct in Co, 33 at. pct in Mo and 18 at. pct in Cr + Si.

A phase analysis has been performed by X-ray diffraction on powder particles. In cobalt alloys, crystalline structures can be either face-centered cubic or hexagonal whereas Laves phases have been found to be hexagonal (Table IV).

Among the phases recalled in Table IV, the following phases were identified in the powder (Figure 4):

- (i) Laves phases of hexagonal close packed structure (hcp)
- (ii) Cobalt solid solution of face-centered cubic (fcc) structure

### B. Consolidation by Spark Plasma Sintering (SPS)

In order to target the parameters of the SPS and HIP cycles, studies of compaction of cobalt powders by SPS have been identified. These studies are related to the

**Table III. Chemical Composition Measured by SEM/EDX on Powders and Bulk Compacts**

		Co	Cr	Mo	Si
As-Atomized Powder					
Laves Phases	(wt pct)	50.0	7.5	38.4	4.2
	(at. pct)	55.1	9.3	26.0	9.6
Solid Solution	(wt pct)	68.0	10.3	20.0	1.6
	(at. pct)	71.4	12.2	12.9	3.5
SPS at 1050 °C					
Laves Phases	(wt pct)	52.7	7.6	35.9	3.6
	(at. pct)	58	9.5	24.2	8.4
Solid Solution	(wt pct)	68.9	11.0	18.1	1.6
	(at. pct)	71.9	13.0	11.6	3.5
HIP at 1050 °C					
Phases Laves	(wt pct)	47.9	6.5	41.6	4.1
	(at. pct)	52.8	8.1	28.2	9.4
Solid Solution	(wt pct)	67.0	11.0	20.0	1.8
	(at. pct)	69.9	13.0	12.8	4.0

biomedical grade CoCrMo ASTM F75, at 28 pct wt Cr and 6 wt pct Mo. The first HIP cycle studies carried out on CoCrMo are very limited in details.<sup>[15,16]</sup> More recently, HIP was also used as a post-treatment to remove residual pores from structures manufactured by additive manufacturing of ASTM 75 grade: for example at 1200 °C for 4 hours at a pressure of 1000 bar.<sup>[17]</sup>

SPS was used by Patel *et al.*<sup>[18]</sup> in the temperature range 1050 °C to 1175 °C, pressures 75 to 100 MPa and holding times of 3 to 10 minutes. The heating and cooling rates applied were 50 and 130 °C min<sup>-1</sup>, respectively. Density of compacts measured by Archimedes method was 8.8978 g/cm<sup>3</sup>, close to the one of the alloy 8.95 g/cm<sup>3</sup>. SPS thus allowed to get a compact with a relative density of 99 pct.

Vickers hardness was HV5 = 800 ± 10 (standard deviation for the indentation line along the diameter).

Same hardness was found in the thickness of the sample. Rockwell hardness was found to be 62.2 HRC.

These values are higher than those of cast Tribaloy: Xu *et al.* found 55 HRC after casting and even lower after heat treatment,<sup>[14]</sup> whereas another study found 55 HRC after casting of a 8.5 wt pct Cr T400 alloy.<sup>[15]</sup>

Figure 5 describes the microstructure of the sample processed by SPS at 1050 °C for 10 minutes, which consists in a homogeneous mix of Laves phases (in white) and cobalt solid solution (in gray). There is a very low visible porosity around the old powder particles whose contours can be guessed thanks to the few pores ( $D < 1 \mu\text{m}$ ).

Fraction of Laves phase was 57.2 ± 2.2 pct after SPS. Eutectic aggregate present after atomization can no longer be distinguished. EDX analyses were performed on a area containing both Laves phases and cobalt solid solution (Figure 6). After SPS, Cr content is 11.0 wt pct in cobalt solid solution and 7.6 wt pct in Laves phases (Table III). Laves phases composition is thus close to Co<sub>3</sub>Mo<sub>2</sub>(Si + Cr), which corresponds to 50 at. pct in Co, 33 at. pct in Mo and 18 at. pct in Cr + Si.

This technique made it possible to obtain, by a 45-minute cycle including 10 minutes at 1050 °C, a material that is more than 99 pct dense. It has shown that it is possible to obtain by powder metallurgy a homogeneous microstructure composed of about 55 pct Laves phases and 45 pct Cobalt solid solution. The Laves phases have a chemical composition close to

**Table IV. Crystalline Phases Available for Diffractometer Brücker**

Name/Formula	Crystallographic System	Lattice Parameter (Angstrom)	Angles	Space Group
Cobalt (cfc)/Co	FCC	$a = b = c = 3.54470$	$\alpha = \beta = \gamma = 90 \text{ deg}$	Fm3m (225)
Cobalt (hcp)/Co	HCP	$a = b = 2.50310$ $c = 4.06050$	$\alpha = \beta = 90 \text{ deg}$ $\gamma = 120 \text{ deg}$	P63/mmc (194)
Solide Solution/ Cr-Co-Mo-Ni	FCC	$a = b = c = 3.60820$	$\alpha = \beta = \gamma = 90 \text{ deg}$	Fm3m (225)
Laves phases/Co <sub>3</sub> Mo <sub>2</sub> Si	HCP	$a = b = 4.70000$ $c = 7.67000$	$\alpha = \beta = 90 \text{ deg}$ $\gamma = 120 \text{ deg}$	P63/mmc (194)
Co carbide/CoC <sub>x</sub>	Cubic	$a = b = c = 3.60610$	$\alpha = \beta = \gamma = 90 \text{ deg}$	P43m (215)

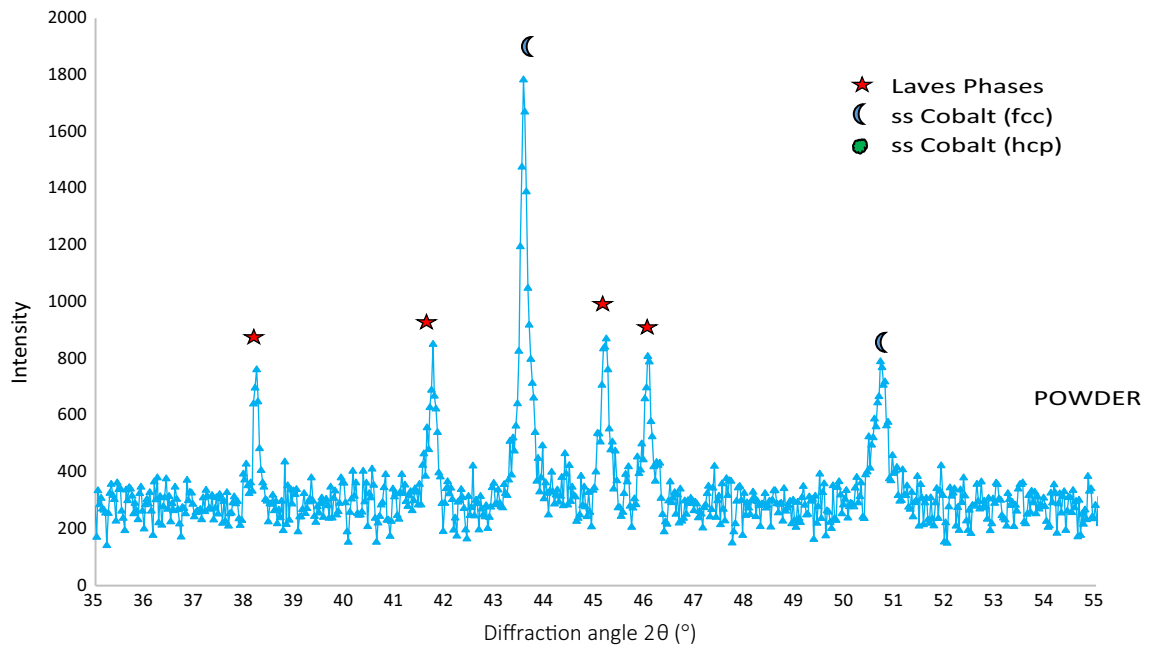


Fig. 4—X-ray diffractogram of T400 atomized powder.

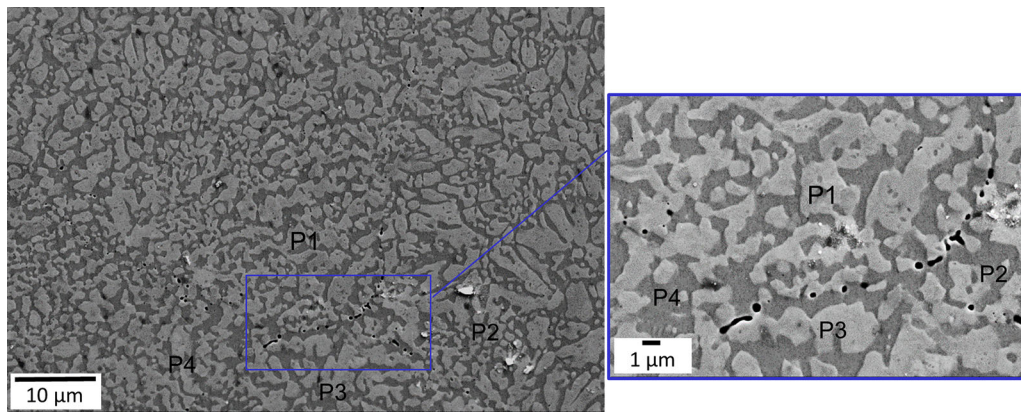


Fig. 5—SEM image (AsB) showing the porosity at the contours of the powder particles noted P1 to P4.

$\text{Co}_3\text{Mo}_2$  (Si + Cr), so *a priori* similar to what can be obtained by casting. The hardness of the sample is 62 HRC, which is higher than a T400 casting whose hardness is generally 55 HRC.

### C. Hot Isostatic Pressing

HIP was performed at 1323 K (1050 °C) for 2 hours and 1433 K (1160 °C) for 3 hours. Parameters were chosen from literature depicting hot pressing of cobalt base alloys such as Stellite HIPed between 1065 °C (Stellite 712) and 1120 °C (Stellite 694).<sup>[15,16]</sup> The cycle is divided into a 10 °C min<sup>-1</sup> heating ramp before 2 hours at 1050 °C under 1020 bar and rapid cooling. The pressure is applied by regular injection of argon into the enclosure, so that the maximum pressure is reached when the maximum temperature is reached. From the billets obtained, a electric discharge machining (EDM)

was carried out to extract the useful material (alloy T400) and machine specimens for mechanical testing:

- two Charpy (impact test) specimens
- parallelepipedic parts to carry out metallurgical characterization (hardness, density, microstructure).

The difference in relative density (Table V) of 0.3 pct between the two billets is less than the uncertainty associated with the method (~ 0.5 pct). However, on both samples A and B, a slightly higher density for the billet HIPed at 1160 °C is observed, which is in line with the reduction in porosity with the increase in cycle temperature and holding time. A higher hardness of the C11262 billet processed at 1050 °C with a hardness of 62.3 HRC (HV5 = 780 ± 20) is observed compared to

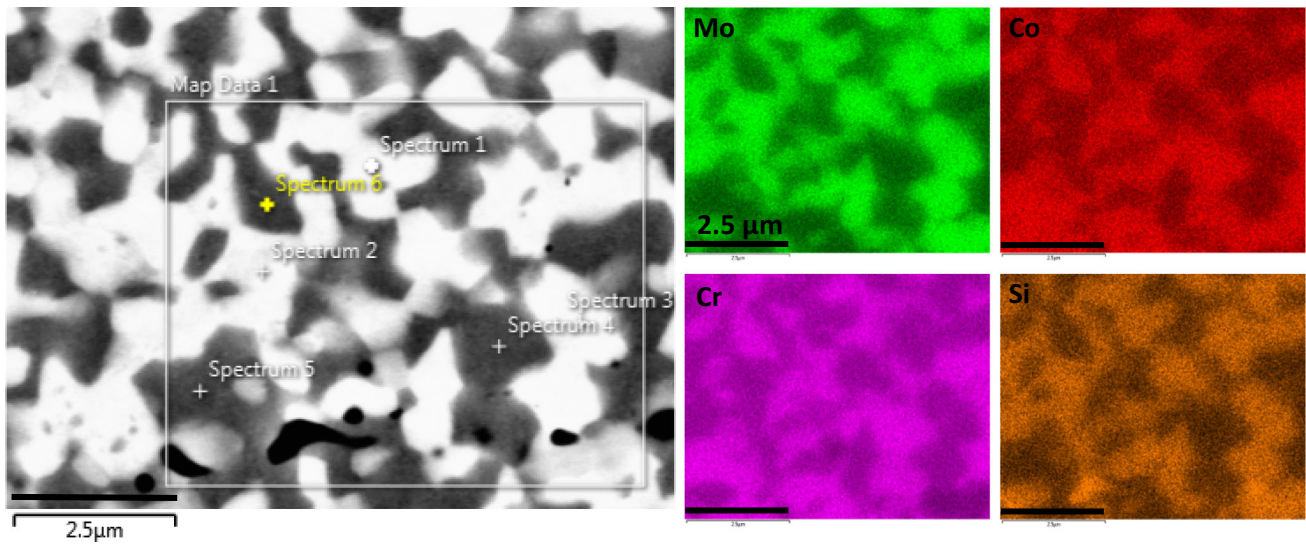


Fig. 6—Area of Spark Plasma Sintered sample analyzed by EDX and corresponding mapping of Mo, Cr, Si and Co contents (pixel intensity increases with content).

**Table 5. Density of HIPed Compacts Measured by Archimedes Method**

Billet Number	C11264	C11262
HIP Conditions	1160 °C—3 h	1050 °C—2 h
Density ( $\text{g cm}^{-3}$ )	$8.93 \pm 0.005$	$8.90 \pm 0.005$
Relative Density (Pct)	99.8	99.5

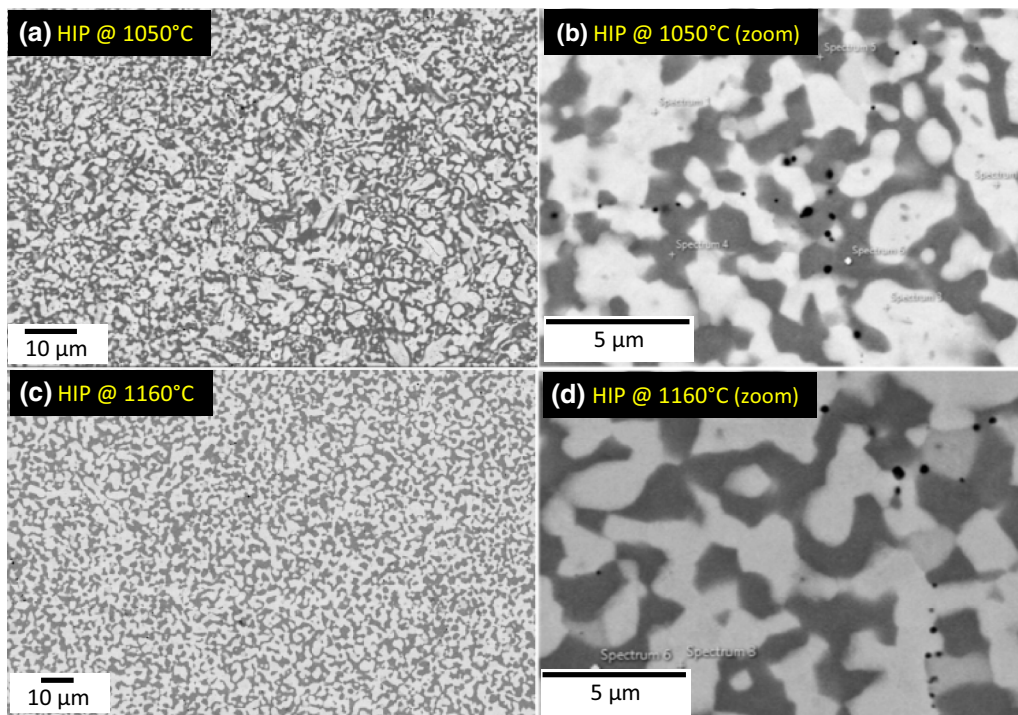


Fig. 7—SEM image (AsB) showing the microstructures of HIPed samples at (a to b) 1050 °C and (c to d) 1160 °C.

a hardness of 61.1 HRC ( $HV5 = 740 \pm 20$ ) for the C11264 billet made at 1160 °C.

Figure 7 shows that the microstructure after compaction at 1160 °C for 3 hours is homogeneous and has almost no residual porosity. Image analysis leads to a Laves phase fraction of 55.8 pct after HIPing at 1050 °C, and 57.1 pct after HIPing at 1160 °C, which is close to what was found after SPS (57.2 pct).

In addition, the Laves phases present are more rounded in the microstructure after HIPing at 1160 °C. The phase boundaries between cobalt solid solution and Laves phase are significantly less acute than in powder or after SPS, highlighting the greater diffusion of alloying elements at the interfaces.

EDX analysis was performed on an area containing both phases whose compositions are reported in Table III.

Impact energies were measured on V-notch Charpy specimens, giving rise to an impact energy of  $1 \pm 0.3$  J depending on the compact, which highlights the very low toughness of all compacts. V-Notch type impact

specimens are severe for brittle materials, which does allow a quantitative comparison between the different compacts. The fracture surfaces of the impact test specimens (Figure 8) confirm this brittleness, with a transgranular cleavage fracture mode. HIPing has resulted in billets that are more than 99 pct dense. SEM imaging reveals a absence of microporosities at the interfaces of powder particles, particularly for the higher temperature cycle (1160 °C, 3 hours).

HIPed materials have microstructures that are quite similar to each other and close to the microstructure of the material after SPS. They have a homogeneous microstructure composed of about 55 pct Laves phases and 45 pct Co solid solution. The Laves phases have a chemical composition close to  $Co_3Mo_2$  (Si + Cr), so *a priori* similar to what can be obtained by casting.

The hardness of the sample is about 800 HV, or 62 HRC, which is higher than a T400 casting whose hardness is generally 55 HRC. However, this high percentage of Laves phases is also at the origin of a near absence of ductility at room temperature.

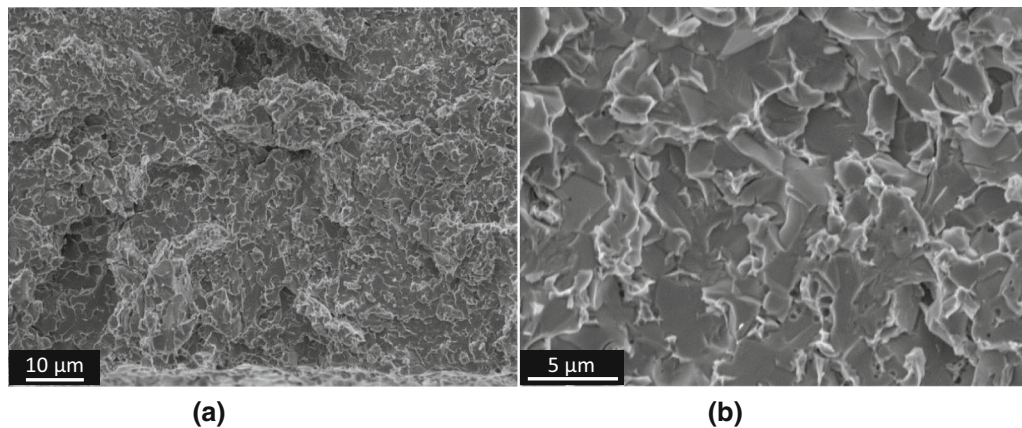


Fig. 8—(a to b) SEM images of fracture surfaces of impact specimens showing a cleavage transgranular fracture mode.

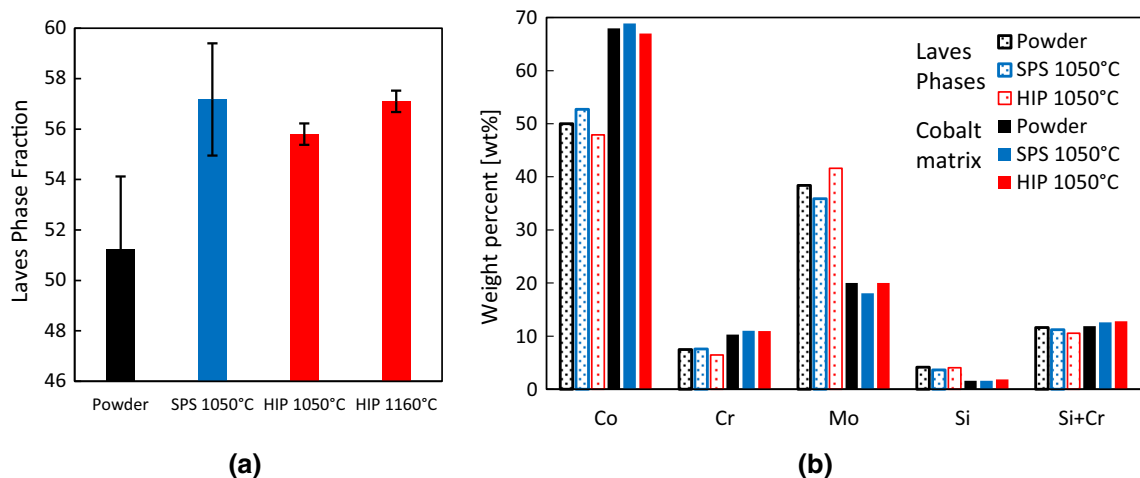


Fig. 9—Laves phase (a) fraction and (b) composition in as-atomized powders and various compacts.



#### IV. DISCUSSION

The compacted powder and materials have a two-phase microstructure composed of a solid cobalt solution reinforced by a Laves phase. The amount of Laves phase varies from 51 pct for atomized powder to 57 pct for HIP at 1160 °C (Figure 9).

Laves phase average composition is 50.2 wt pct (55.6 at. pct) Co, 38.6 wt pct (26.3 at. pct) Mo, 7.2 wt pct (9.0 at. pct) Cr and 4.0 wt pct (9.2 at. pct) Si, very close to the Laves phase  $\text{Co}_3\text{Mo}_2(\text{Si} + \text{Cr})$ , and varies very little with the high-temperature consolidation cycle. This phase was also identified by X-ray diffraction from the atomized state to the materials consolidated by HIP, as shown in Figure 10. We notice an evolution in the

diffraction peaks, *a priori* markers of the transition from a cubic face-centered phase (fcc) in the powder to a mixture of phases (fcc) with a hexagonal phase (hcp), which has been already observed.<sup>[19]</sup>

The impact tests showed a brittle behavior of the materials consolidated by HIP, either at 1050 °C or 1160 °C. This behavior can be explained by the presence of a high fraction of Laves phases, which also explains the hardness of about 62 HRC. Considering the nano-indentation study of Wu, the hardness of the Laves phases and the eutectic phase of a T400 alloy obtained by casting are respectively 7.5 GPa and 21.8 GPa).<sup>[14,20]</sup> Nano-indentation could not be performed in this study.

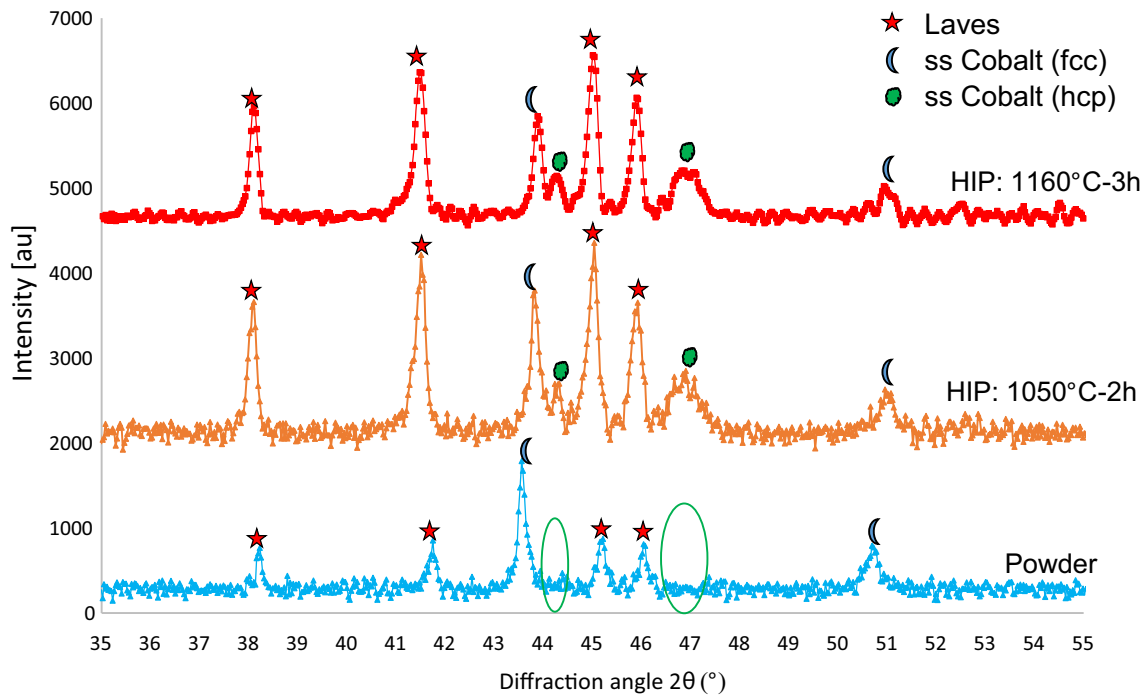


Fig. 10—Evolution of the phases identified by X-ray diffraction.

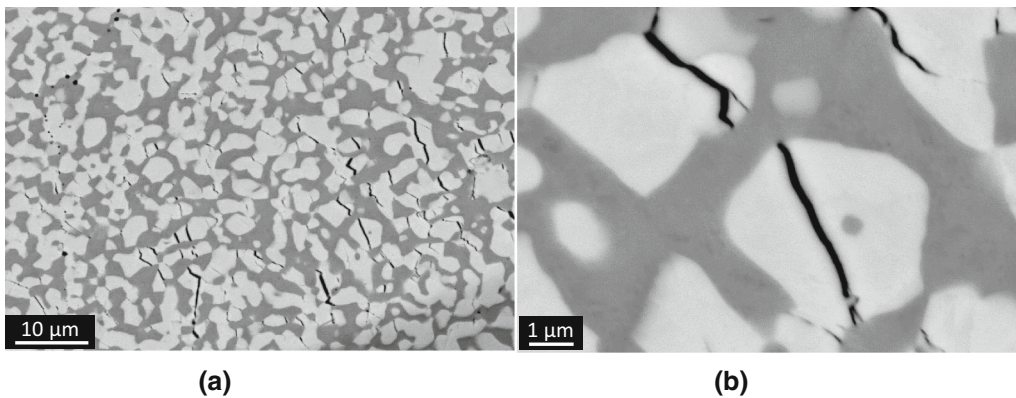


Fig. 11—SEM (backscattered electron) images of cracks (a) near a hardness indent, (b) zoom on a crack shearing several particles of Laves phases but being stopped, in the observed plane, by the cobalt matrix.

If one considers the cracking mechanisms of T400 obtained by powder metallurgy, one can clearly see the role of the matrix in stopping cracks that spread easily in the hard and fragile Laves phases. This is illustrated by different SEM observations around hardness indents made on several samples (Figure 11). It is quite straightforward to conclude that it is necessary to reduce the fraction of particles of Laves phases in order to obtain a better compromise between impact strength and hardness. However, to combine both core ductility and surface hardness, a composition graded materials could be produced by powder metallurgy.

## V. CONCLUSION

This study showed the benefit of powder metallurgy for the manufacture of T400 components, in particular it makes it possible to obtain a material that is more than 99 pct dense and has a fine and homogeneous microstructure.

However, the composition of the starting powder induces a high fraction of Laves phase (> 55 pct), which induces a strong increase in hardness (about 62 HRC) at the expense of the material's toughness.

In order to overcome this lack of ductility, several evolutions shall be studied.

On the one hand, reducing the excessive contents of chromium, silicon and molybdenum, all present in the Laves phases will reduce the fraction of Laves phases in the alloy and thus improve toughness.

On the other hand, a certainly more robust solution for combining core toughness and surface hardness would be the manufacture of a graded material with a chemical composition. The technological paths envisaged would be either powder metallurgy by compaction of several powder beds powders or direct manufacturing processes, such as direct metal deposition (DMD) or direct-ink writing.

## ACKNOWLEDGMENTS

X. Boulnat thanks S. Cottrino and F. Mercier for their help in performing high-temperature consolidations of the powders.

## REFERENCES

1. I. Hutching and P. Shipway: *Tribology: Friction and Wear of Engineering Materials*, 2nd ed., Butterworth-Heinemann, Oxford, 2016.
2. G. Boellia, V. Cannillo, L. Lusvardia, M. Montorsia, F.P. Mantinia, and M. Barletta: *Wear*, 2007, vol. 263, pp. 1397–16.
3. T. Sahraoui, H.I. Feraoun, N. Fenineche, G. Montavon, H. Aourag, and C. Coddet: *Mater. Lett.*, 2004, vol. 58 (19), pp. 2433–36.
4. J.Y. Cho, S.H. Zhang, T.Y. Cho, J.H. Yoon, Y.K. Joo, and S.K. Hur: *J. Mater. Sci.*, 2009, vol. 44, pp. 6348–55.
5. Hogan. [https://www.hoganas.com/globalassets/media/sharepoint-documents/brochuresanddatasheetsalldocuments/powder\\_choice\\_with\\_ease.pdf](https://www.hoganas.com/globalassets/media/sharepoint-documents/brochuresanddatasheetsalldocuments/powder_choice_with_ease.pdf), 2018.
6. Kennametal. <https://www.kennametal.com/en/products/powdered-materials-and-equipment/thermal-spray-powders.html>, 2018.
7. K. Jiang, R. Liu, K. Chen, and M. Liang: *Wear*, 2013, vol. 307, pp. 22–27.
8. A. Frenk and W. Kurz: *Wear*, 1994, vol. 174, pp. 81–91.
9. C.D. Opris, R. Liu, M.X. Yao, and X.J. Wu: *Mater. Des.*, 2007, vol. 28, pp. 581–91.
10. M.A. Ashworth, J. Bryar, M.H. Jacobs, and S. Davies: *Powder Metall.*, 1999, vol. 42, pp. 243–49.
11. A. Halstead and R.D. Rawlings: *J. Mater. Sci.*, 1985, vol. 20, pp. 1248–56.
12. E. Ström, J. Zhang, S. Eriksson, C. Li, and D. Feng: *Mater. Sci. Eng A*, 2002, vols. 329–331, pp. 289–94.
13. R. Liu, W. Xu, M.X. Yao, P.C. Patnaik, and X.J. Wu: *Scripta Mater.*, 2005, vol. 53, pp. 1351–55.
14. W. Xu, Master's thesis, Carleton University, 2005.
15. F.S. Georgette and J.A. Davidson: *J. Biomed. Mater. Res.*, 1986, vol. 20, pp. 1229–48.
16. T.J.J. Jacobs, R.M. Latanision, T.R.M. Rose, and S.J. Veeck: *J. Orthop. Res.*, 1990, vol. 8, pp. 874–82.
17. J. Haan, M. Asseln, M. Zivcec, J. Eschweiler, R. Radermacher, and C. Broeckmann: *Powder Metall.*, 2015, vol. 58, p. 161.
18. B. Patel, F. Inam, M. Reece, M. Edirisinghe, W. Bonfield, J. Huang, and A. Angadji: *J. R. Soc. Interface*, 2010, vol. 7, pp. 1641–45.
19. Q. Meng, S. Guo, X. Zhao, and S. Veintemillas-Verdaguer: *J. Alloy. Compd.*, 2013, vol. 580, pp. 187–90.
20. W. Xu, R. Liua, P.C. Patnaik, M.X. Yao, and X.J. Wu: *Mater. Sci. Eng. A*, 2007, vol. 452, pp. 427–36.

**Publisher's Note** Springer Nature remains neutral with regard to jurisdictional claims in published maps and institutional affiliations.